Multivariate nonstationary modeling of cerebral hemodynamics

Kyriaki Kostoglou, Chantel T. Debert, Marc J. Poulin and Georgios D. Mitsis

***Abstract*— We extracted adaptive univariate and multivariate dynamic models of cerebral hemodynamics during resting and hypercapnic conditions using a Recursive Least Squares estimation scheme with multiple adaptive forgetting factors. The time dependent relationship between mean arterial blood pressure (MABP), end-tidal CO2 tension (P_{ETCO2}) and middle cerebral artery blood flow velocity (CBFV) was assessed using Laguerre - Volterra models with time varying coefficients. The results suggest that the addition of P_{ETCO2} as a second input yields more accurate and less nonstationary estimates, indicating that unobservable physiological variables are important in the context of nonstationary systems modeling, and particularly for assessing cerebral hemodynamics and autoregulation.**

I. Introduction

Cerebral autoregulation is a complex homeostatic mechanism that helps the brain maintain relatively constant cerebral blood flow (CBF) and oxygen supply, despite variations in a number of external physiological factors such as arterial blood pressure (ABP). During impaired autoregulation, abnormal changes in CBF can lead to cerebral hyperaemia, ischemia or even stroke. Transfer function analysis [1] has revealed a close relationship between CBF velocity (CBFV) and ABP for frequencies over 0.07Hz. Below this limit, low coherence values between ABP and CBFV suggest that nonlinearities, nonstationarities or other external physiological factors may also contribute to effective blood flow stabilization.Previous studies of cerebral autoregulation have employed multivariate models that incorporate ABP and carbon dioxide (CO_2) as inputs [2-6]. CO_2 is known to have a profound effect on CBF. Hypercapnia causes dilation of cerebral arteries and increases blood flow, whereas hypocapnia leads to arterial constriction and decreased flow. Moreover, the role of nonstationarities has been recently highlighted in a number of studies [7-13]. In the present study, we extend the results presented in [13] by investigating the role of time-varying behavior both during resting conditions as well as during hypercapnia. To do this, we employ a multivariate adaptive data-driven approach that employs discrete-time, time-varying Laguerre-Volterra models [14-16].

Kyriaki Kostoglou is with the Department of Electrical and Computer Engineering, University of Cyprus, Nicosia, Cyprus (e-mail: kostoglou.kyriaki@ucy.ac.cy).

Chantel T. Debert is with the Department of Physical Medicine and Rehabilitation, Faculty of Medicine, University of Calgary, AB, Canada (e-mail: ctdebert@ucalgary.ca).

Marc J. Poulin is with Department of Physiology & Pharmacology, Faculty of Medicine, University of Calgary, AB, Canada, the Department of Clinical Neurosciences, Faculty of Medicine, University of Calgary, AB, Canada, the Faculty of Kinesiology, University of Calgary, AB, Canada, the Hotchkiss Brain Institute, Faculty of Medicine, University of Calgary, AB, Canada and Libin Cardiovascular Institute of Alberta, Faculty of Medicine, University of Calgary, AB, Canada (e-mail: poulin@ucalgary.ca).

Georgios D. Mitsis is with the Department of Bioengineering, McGill University, Montreal, Quebec, Canada (corresponding author; e-mail: georgios.mitsis@mcgill.ca)

II. Mathematical Methods

A. Multiple Input Single Output Discrete-Time Volterra Model

The relationship between MABP, P_{ETCO2} and CBFV can be expressed using a discrete-time Volterra model. Volterra models are very useful for system representations due to their nonlinear structure and their property of linearity with respect to their parameters. The Q-th order, nonlinear, two-input, single-output relationship of a dynamic and causal system can be written as [14],

$$y(n) = k0 + \sum_{i=1}^{2}\sum_{m} {k_1}^{(x_i)}(m)x_i(n-m) + \sum_{i_1,i_2=1}^{2}\sum_{m_1,m_2} {k_2}^{(x_{i_1},x_{i_2})}(m_1,m_2)x_{i_1}(n-m_1)x_{i_2}(n-m_2) + \cdots + \sum_{i_1..i_Q=1}^{2}\sum_{m_1..m_Q} {k_Q}^{(x_{i_1},\ldots,x_{i_Q})}(m_1,\ldots,m_Q)x_{i_1}(n-m_1)\ldots x_{i_Q}(n-m_Q)$$

where x_i are the inputs, $y(n)$ is the output and k_Q are the Q-th order Volterra kernels of the system. The first-order Volterra system corresponds to the convolution sum for a linear system. Higher-order kernels can be viewed as weighting functions that describe the effect of past input values, as well as the effect of the Q-th order products between past values of each input and different inputs in order to generate the output signal. Often, the system kernels are projected onto an orthornormal basis of discrete-time Laguerre functions (DLFs) [14]. The least-squares technique may be then used in order to compute the expansion coefficients. The Laguerre parameters a_i $(0 < a_i < 1)$ define the time scale for which the expansion of the system kernels is most efficient in terms of convergence. Systems with fast dynamics (small memory) require a small a_i (close to 0), whereas systems with slow dynamics (large memory) require a large one (close to 1). Choosing an appropriate value for these parameters is crucial as it affects model accuracy and complexity. We use a different parameter for each input, as different inputs are typically characterized by different dynamic characteristics.

978-1-4244-7929-0/14/$26.00 ©2014 IEEE

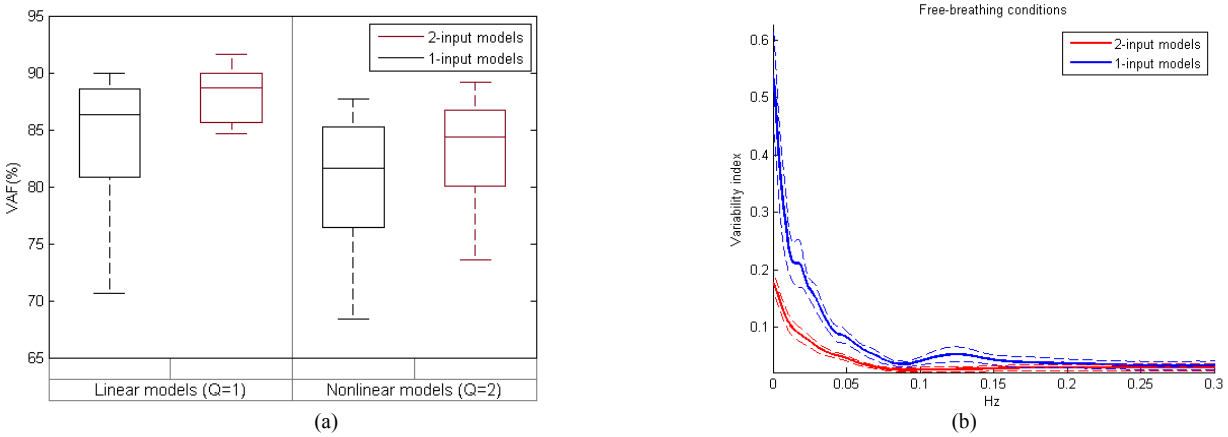

Figure 1: (a) Variance Accounted For (VAF%) boxplots of the model predictions for all subjects and (b) mean variability indices of the MABP kernels (solid line +/- standard error of the mean – dashed lines) as a function of frequency for one-input and two-input linear models under free-breathing conditions. For the linear case, the differences in VAF% between one-input and two-input models are significantly. Moreover, one-input models exhibit higher variability in the low and very low frequency range (0-0.15Hz)

B. Recursive Least Squares with Multiple Forgetting Factors

Time dependent model parameters can be adequately tracked and estimated using adaptive algorithms like Recursive Least Squares (RLS). The standard RLS formulation includes a constant forgetting factor (FF) $\lambda \in (0,1]$ that discards gradually older data in favor of more recent information. However, in a multiple input system parameters corresponding to different inputs may vary with different rates. In order to be able to more accurately track possible variations, we applied a multiple adaptive forgetting factor scheme. Each input was assigned with a unique time-varying λ_i that took into account the influence of the new data using Cook's distance [15]. The update equations for the unknown coefficients vector at time point t are written as [16]:

$$e(t) = y(t) - \boldsymbol{\varphi}^{\boldsymbol{T}}(t)\hat{\boldsymbol{c}}(t-1)$$

$$r(t) = \boldsymbol{\varphi}^{\boldsymbol{T}}(t)\boldsymbol{P}(t-1)\boldsymbol{\varphi}(t)$$

$$\boldsymbol{K}(t) = \frac{\boldsymbol{P}(t-1)\boldsymbol{\varphi}(t)}{1+r(t)}$$

$$\hat{\boldsymbol{c}}(t) = \hat{\boldsymbol{c}}(t-1) + \boldsymbol{K}(t)e(t)$$

$$\boldsymbol{W}(t) = \boldsymbol{P}(t-1) - \frac{\boldsymbol{P}(t-1)\boldsymbol{\varphi}(t)\boldsymbol{\varphi}^{\boldsymbol{T}}(t)\boldsymbol{P}(t-1)}{1+r(t)}$$

$$\boldsymbol{P}(t) = \boldsymbol{\Lambda}(t)\boldsymbol{W}(t)\boldsymbol{\Lambda}(t) \quad (\in \boldsymbol{R}^{n\times n})$$

$$\boldsymbol{\Lambda}(t) = diag\left(\sqrt{\frac{1}{\lambda_i(t)}}\right)$$

where n is the total number of coefficients, $e(t)$ is the output prediction error, $\boldsymbol{\varphi}(t)$ is the regressor corresponding to time t, $\boldsymbol{K}(t)$ is the gain matrix and $\boldsymbol{P}(t)$ is the covariance matrix of the coefficient estimates. The initial value for this matrix is $\boldsymbol{P}(0) = \rho \boldsymbol{I}_{n\times n}$, where ρ in this case was selected to be 10^4. The elements of $\boldsymbol{P}(t)$ that belong to the i-th input are assigned with a unique time varying FF $\lambda_i(t)$.

C. Model order selection

Model order selection is the task of selecting a specific model structure in order to avoid overfitting and poor predictive performance in new datasets. However, in nonstationary systems we are more interested in tracking possible changes and building a model that can adequately approximate the underlying mechanisms which are changing with time. For each dataset, we applied the aforementioned RLS scheme and we selected the model structure and the FFs that globally minimized statistical criteria such as the Bayesian and Akaike Information criteria (BIC and AIC) using a mixed integer Genetic Algorithm [17,18]. A Genetic algorithm (GA) is an adaptive stochastic optimization algorithm based on the idea of natural evolution that can be used to solve various optimization problems. Both discrete (integer) and continuous (floating point) variables are taken into account, hence the term mixed-integer GA.

III. Experimental Data

The subjects gave informed consent to participate in this study, which was approved by the University of Calgary Conjoint Health Research Ethics Board. ABP was monitored by finger photoplethysmography, CBFV was measured in the right middle cerebral artery using transcranial Doppler ultrasonography, while P_{ETCO2} was measured by mass spectrometry. 40 minutes of beat-to-beat values of ABP and CBFV, as well as breath-to-breath values of P_{ETCO2} were obtained from thirteen healthy subjects under free-breathing conditions. Furthermore, we also analysed data from 8 female subjects during 10 minutes of baseline and 20 minutes of sustained euoxic hypercapnia in order to track cerebral hemodynamics during an externally induced CO2 stimulus. Arterial gas tensions were controlled using dynamic end-tidal forcing. All experimental variables were interpolated and resampled at 1Hz to obtain equally spaced time series data.

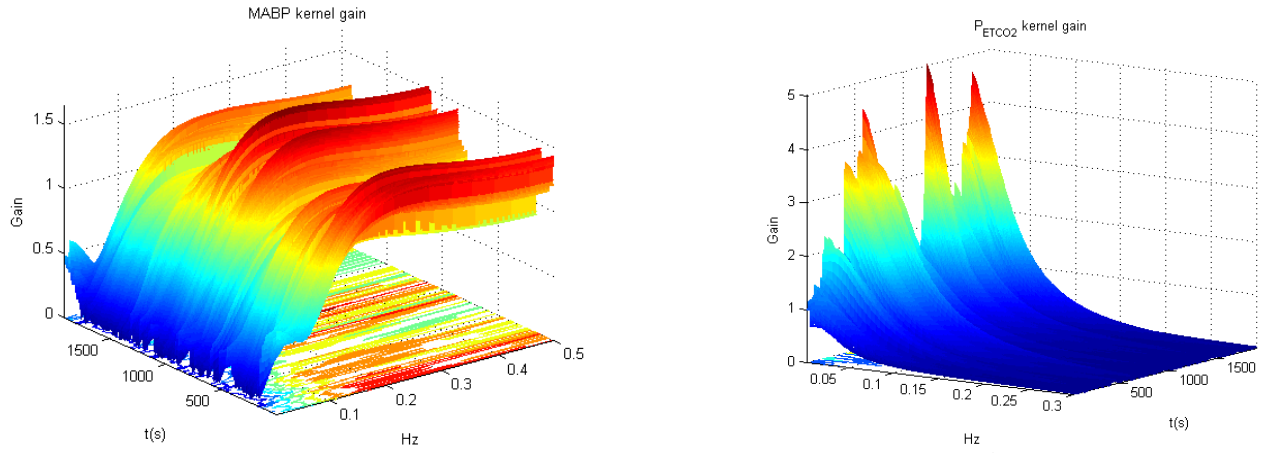

(a) (b)

Figure 2: 1st-order kernels for one representative subject under free-breathing conditions in the time-frequency domain (a) MABP and (b) P_{ETCO2} kernels for a two-input model.

IV. Results

A. Free-breathing conditions data

Single and multiple adaptive forgetting factor schemes were applied to one and two input ($input_1$: MABP, $input_2$: P_{ETCO2}, output: CBFV) models respectively. Based on the identified time-varying systems from all subjects, two-input models achieved a higher predictive performance (Fig.1a) and exhibited less time-varying characteristics compared to one-input models (Fig.1b). The amount of nonstationarity in a system is correlated to the obtained values of the FFs. Lower FFs usually indicate the presence of rapid system changes, whereas FFs closer to one describe systems with slow variations. Lower FFs can also indicate the absence of crucial information that can lead to more stable parameter estimation. In order to justify this, we computed the variability of the identified one-input MABP-CBFV kernels in the frequency range of interest (0-0.5Hz) and we detected high variability in the very low frequency range, where P_{ETCO2} and CBFV are correlated (Fig.1b). The variability index of each extracted time-varying kernel was computed as [10, 13],

$$VI_{x_i}(f) = \frac{\frac{1}{N-1}\sum_{t=1}^{N}\left(p_t(f) - \bar{p}(f)\right)^2}{\bar{p}(f)}$$

where $p_t(f)$ is the FFT magnitude of the first-order kernel of the input x_i for time t of the data segment at frequency f and $\bar{p}(f)$ is the average value of $p_t(f)$ over t at each frequency f. For all subjects, P_{ETCO2} kernels exhibited a more random and variable pattern compared to the MABP kernels (Fig.2). The origin of these nonstationary characteristics may be partially due to the low correlation between P_{ETCO2} and CBFV at specific time windows, as well as to the possible presence of a time-varying pure time delays between P_{ETCO2} and CBFV as suggested by Fig. 3, where we show the windowed cross-correlation function between P_{ETCO2} and CBFV as a function of time. Note that in the present study we assumed that this delay was constant (4sec) for each subject. Low correlation may affect the estimation procedure and the update of the covariance matrix in the RLS algorithm and time-varying delays are translated into time-varying model orders, since the model order complexity needs to be increased in case of large pure time delays and decreased in case of small or no delays.

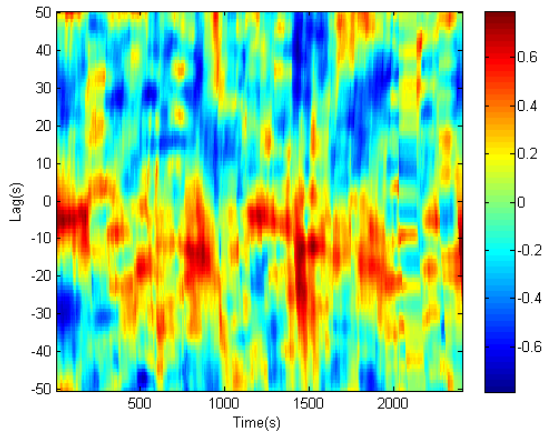

Figure 3: Normalized windowed cross correlation between P_{ETCO2} and CBFV. The pure time delay of the effects of P_{ETCO2} is variable, assuming values between 5 and 15 sec. Time windows with low cross correlation are also evident.

A. Hypercapnic step data

10 minutes of baseline period were followed by a 20 minutes hypercapnic step and a 10 minutes post-hypercapnic phase. Our main goal was to extract and quantify important features of the identified nonstationary system such as phase and gain through time and provide a more comprehensive characterization of dynamic autoregulation [13]. Based on all subjects we found that the phase lead of the MABP component in the low frequency range decreased during the hypercapnic step, indicating impaired autoregulation (Fig.4a). This phenomenon was accelerated during the onset of the step and decelerated afterwards. On the contrary, during free breathing conditions, the phase lead exhibited periodicities around specific values (Fig.4b).

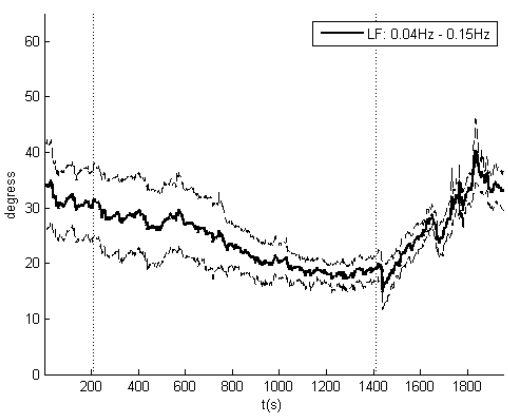

(a)

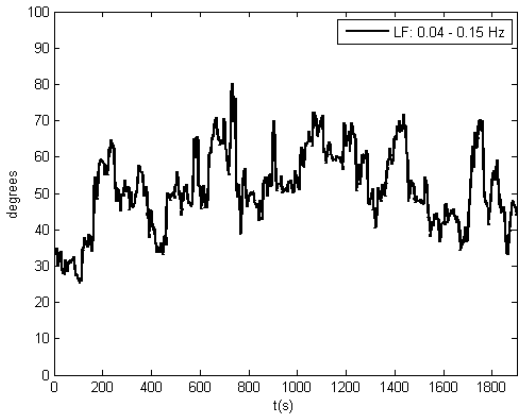

(b)

Figure 4: (a) Averaged (solid line +/- standard error of the mean – dashed lines) over all subjects (a) mean phase of the MABP kernels in the low frequency range (LF: 0.04-0.15 Hz) for two-input models as a function of time during the three experimental phases (baseline, hypercapnia and post-hypercapnia). The two vertical dashed lines denote the onset (around 200s) and the offset (around 1400s) of the hypercapnic step (b) Mean phase of a representative 1st-order MABP kernel (Fig. 2a) in the low frequency range (LF: 0.04-0.15 Hz) for a two-input model as a function of time under free-breathing conditions.

We also identified a significantly faster increase in the phase lead of the system during and after the offset of the hypercapnic step (Fig.4a). The gain of the MABP component decreased abruptly immediately after the onset of the hypercapnic step but rebounded to its baseline values. Overall we did not observe any specific pattern. The variability indices of the extracted MABP kernels were higher for the one-input models during all three experimental phases [13] indicating once again that the addition of P_{ETCO2} results into less time-varying components.

V. Discussion And Conclusions

We investigated cerebral autoregulation under free-breathing and hypercapnic conditions by applying a multivariate data-driven adaptive approach. One input models exhibited in general less accurate and more time-varying characteristics compared to two-input models indicating that P_{ETCO2} plays an important role mainly in the very low frequency range. During resting conditions, time-varying forgetting factors revealed periodicities in the MABP kernel components, whereas the P_{ETCO2} kernels varied in a more random pattern. The origin of these nonstationarities is an interesting subject that needs to be examined further. In accordance with previous studies, sustained euoxic hypercapnia led to a decrease in the phase lead of the MABP component indicating that hypercapnia is associated with impaired cerebral autoregulation.

References

[1] R. Zhang, J. H. Zuckerman, C.A. Giller and B. D. Levine, “Transfer function analysis of dynamic cerebral autoregulation in humans,” American Journal of Physiology - Heart and Circulatory Physiology, vol. 274, no. 1, pp. H233–H241, 1998.

[2] G.D. Mitsis, M.J. Poulin, P.A. Robbins, and V.Z. Marmarelis, “Nonlinear modeling of the dynamic effects of arterial pressure and co2 variations on cerebral blood flow in healthy humans,” Biomedical Engineering, IEEE Transactions on, vol. 51, no. 11, pp. 1932 –1943, 2004.

[3] R.B Panerai, D.M Simpson, S.T. Deverson, P. Mahony, P. Hayes and D.H Evans, “Multivariate dynamic analysis of cerebral blood flow regulation in humans,” IEEE Trans Biomed Eng 47: 419-421, 2000.

[4] G.D. Mitsis, R. Zhang, B.D. Levine, and V.Z. Marmarelis, “Cerebral hemodynamics during orthostatic stress assessed by nonlinear modeling Regulation of the Cerebral Circulation Cerebral hemodynamics during orthostatic stress assessed by nonlinear modeling,” Journal of Applied Physiology, pp. 354–366, 2006.

[5] G.D. Mitsis, R. Zhang, B.D. Levine, E. Tzanalaridou, D.G. Katritsis and V.Z. Marmarelis, "Autonomic neural control of cerebral hemodynamics," Engineering in Medicine and Biology Magazine, IEEE, vol.28, no.6, pp.54-62, 2009.

[6] R.B. Panerai, N.E. Dineen, F.G. Brodie and T.G. Robinson, “Spontaneous fluctuations in cerebral blood flow regulation: contribution of PaCO2,” Journal of Applied Physiology 109 6 1860-8, 2010.

[7] R.B Panerai, P. Eames and J.F. Potter, “Variability of time domain indices of dynamic cerebral autoregulation,” Physiological Measurement, vol. 24, 2003.

[8] N.E. Dineen, F.G. Brodie, T.G. Robinson and R.B. Panerai, “Continuous estimates of dynamic cerebral autoregulation during transient hypocapnia and hypercapnia,” Journal of Applied Physiology 108 3 604-13, 2010.

[9] J. Liu, M.D. Simpson, J. Yan, and R. Allen, “Tracking time-varying cerebral autoregulation in response to changes in respiratory PaCO2,” Physiological measurement, vol. 31, no. 10, pp. 1291–307, 2010.

[10] M.M. Markou, M.J. Poulin and G.D. Mitsis,”Nonstationary analysis of cerebral hemodynamics using recursively estimated multiple-input nonlinear models,” CDC-ECE 2011: 5768-5773, 2011.

[11] V.Z. Marmarelis, D. Shin, M. Orme and R. Zhang. "Time-Varying Modeling of Cerebral Hemodynamics," Biomedical Engineering, IEEE Transactions on , vol.PP, no.99, pp.1,1, 2013.

[12] R.B. Panerai, “Nonstationarity of dynamic cerebral autoregulation,” Medical engineering & physics, 2013.

[13] K. Kostoglou, C.T. Debert, M.J. Poulin, and G.D. Mitsis. "Nonstationary multivariate modeling of cerebral autoregulation during hypercapnia," Medical engineering & physics, 2013.

[14] V.Z. Marmarelis, "Nonlinear Dynamic Modeling of Physiological Systems" Piscataway, NJ: Wiley-Interscience & IEEE Press, 2004.

[15] I. Sánchez, "Recursive Estimation of Dynamic Models Using Cook's Distance, With Application to Wind Energy Forecast," Technometrics, vol. 48, no. 1, pp. 61-73, 2006.

[16] N. Yoshitani and A. Hasegawa, “Model-based control of strip temperature for the heating furnace in continuous annealing,” IEEE Transactions on Control Systems, 6.2.p.146, 1998.

[17] D. Lawrence, “Handbook of genetic algorithms,” Van Nostrand Reinhold, New York, 1991.

[18] K. Deb, “An efficient constraint handling method for genetic algorithms,” Computer Methods in Applied Mechanics and Engineering, 186(2–4), pp. 311–338, 2000.